68th International Astronautical Congress (IAC), Adelaide, Australia, 25-29 September 2017.

IAC-17,C1,4,x37887

Docking of a space tug with upper stage debris object using deployable flexible beam

V. S. Aslanov[a]*, V. V. Yudintsev[b]

[a] *Theoretical mechanics department, Samara National Research University, 34, Moskovskoye shosse, Samara, 443086, Russia*, aslanov_vs@mail.ru
[b] *Theoretical mechanics department, Samara National Research University, 34, Moskovskoye shosse, Samara, 443086, Russia*, yudintsev@classmech.ru
* Corresponding Author

Abstract

A new technique of docking of a space tug with spent non-cooperative orbital stage by using a deployable elastic probe is proposed. The developed mathematical models demonstrate the proposed method and cover primary stages of the relative motion of the space tug and debris, including docking stage and the probe retraction stage. The simulation results demonstrate decreasing the contact-impact forces resulting from the collision of the probe with the debris and increasing the probability of successful docking.

Keywords: space debris, space tug, probe-cone mechanism, flexible beam

1. Introduction

To lower the risk of avalanche-like growth in the debris population, it is necessary to actively remove large-size objects from near Earth orbits. There are a lot of papers proposing active debris removal methods (ADR) [1–6].

One the important phase of the ADR is a capture phase after the final rendezvous of the space tug with the target. The capture technique depends on the target type and its attitude motion. Often, orbital stages are utilizing jet nozzles to create additional forces (with the forces produced by separation devices like spring pushers) for the safe separation from the main payload. This separation procedure can lead to the tumbling of the orbital stage at the end of its lifetime, which makes it difficult for gripping during ADR mission [7,8]. Traditional methods using manipulators are less suitable for such types of debris [9–11] due to possible high dynamics effects during the contact of the space tug gripping mechanism with the tumbling debris. Non-rigid capture techniques can be used to grip tumbling target debris, using for example nets or harpoons [12–14], but these methods require sophisticated control system for the space tug.

One of the proposed methods for gripping spent upper stages involves the use of well-known probe-cone type mechanism [15,16]. In this case, the probe is mounted on a space tug [17] and the nozzle of the upper stage type debris can be used as the "cone" part of a probe-cone docking mechanism [18,19] (Fig. 1).

Docking with tumbling debris using probe-cone mechanism can cause high dynamic loads in the construction of the docking devices [20–22]. It will require an increase in the mass of the mechanisms and complexity of the tug's control system.

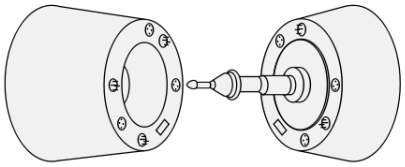

Fig. 1. Probe-cone docking [23]

We suggest that using retractable flexible high-aspect-ratio (long) docking probe reduces the reaction forces caused by the interaction between the elements of the docking device and the nozzle of the debris.

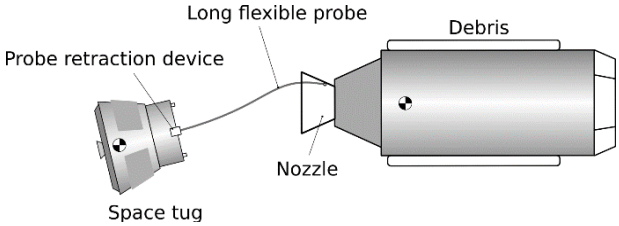

Fig. 2. Docking using long flexible probe

Docking with tumbling debris object using a probe-cone mechanism requires high docking speed to increase the probability of successful docking. It is anticipated, that the long flexible probe is more suitable to the tumbling space debris and to the possible control error of the relative motion of the space tug relative to the debris. The long flexible probe also increases the safety of the gripping process for the space tug due to a greater distance between the space tug and debris.

This paper is devoted to the preliminary analysis of two stages of the ADR using proposed technique including the stage when the tip of the probe slides along the surface of the debris nozzle, and the probe

retraction stage when the tug retracts the beam with the gripped debris.

2. Description of the docking process

The docking process consists of five stages.

1) At the first stage, the space tug approaches to the debris and deploys the flexible probe (Fig. 3a).

2) At the second stage, the flexible probe contacts with the surface of the nozzle. The tip of the probe slides along the nozzle of the space debris (Fig. 3b).

3) At the third stage, the tip of the probe crosses the critical section of the nozzle (Fig. 3c). Successful docking refers to the passage of the probe's tip throw the nozzle throat which initiates the triggering of the latches to fix the tip of the probe in the nozzle.

4) At the fourth stage, the space tug retracts the flexible probe. The distance between the space tug and debris object decreases (Fig. 3d). During this stage, the possible angular motion of the whole system should be stabilized.

5) At the fifth stage, the space tug docks with the debris and the whole system is deorbited or transferred to a graveyard orbit.

a) Terminal rendezvous and probe deployment

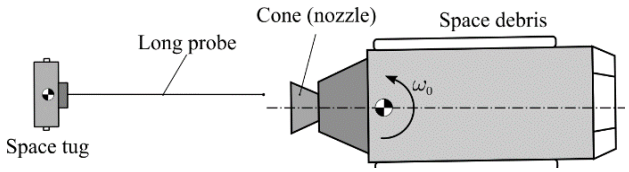

b) Docking

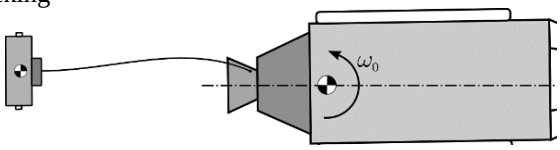

c) Locks the probe tip in the nozzle

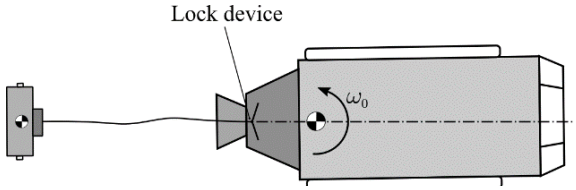

d) Retracting the probe

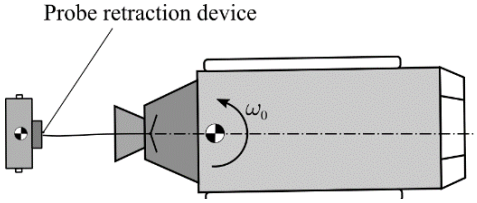

Fig. 3. Docking stages

3. Models

3.1 Docking stage

It is supposed that the docking process is very rapid, that allows us to neglect the influence of the gravitational field and other forces. The scheme of the system is shown in Fig. 4. The space tug and debris are considered as rigid bodies.

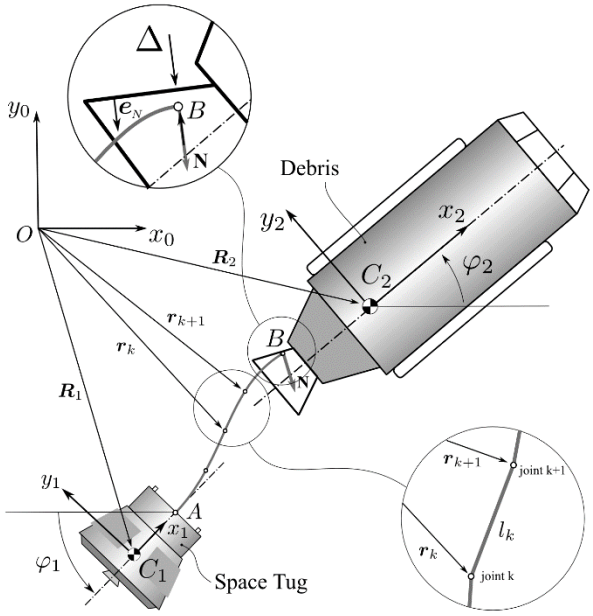

Fig. 4. Model of docking stage

The probe is considered as a chain of rigid bodies connected by elastic joints. The stiffness of k-th joint is

$$c_{\varphi k} = \frac{EJ}{l_k} \tag{1}$$

In a first approximation, we neglect energy losses and assume that there is no damping in the system.

The contact interaction between the tip of the probe and the nozzle surface is modelled using contact force which depends on the penetration depth Δ (Fig. 4)

$$\boldsymbol{N} = \begin{cases} 0, & \Delta > 0 \\ \boldsymbol{e_N} N(\Delta, \dot{\Delta}), & \Delta \le 0 \end{cases} \tag{2}$$

where $\boldsymbol{e_N}$ is the unit vector perpendicular to the surface of the nozzle, $N(\Delta, \dot{\Delta})$ is the contact force

$$N(\Delta, \dot{\Delta}) = c_N \Delta + k_N \dot{\Delta} \tag{3}$$

where c_N and k_N are the contact stiffness and damping. The nozzle is represented as a conical surface. The model of the considered system during docking is built using MSC.ADAMS simulation software.

3.2 Probe retraction stage

After successful docking and locking of the probe tip in the nozzle of the space debris, we get two bodies connected with the flexible probe. This system is considered as an uniform Euler–Bernoulli beam with tip masses and inertia [24]. We suppose that the retraction speed is slow so the dynamic effects due to shortening of the probe is neglected. To preliminary analysis of the motion of the probe during the retraction phase, we trace the variations of the frequency and shapes of the probe oscillations when the length of the probe is decreasing.

The equation of motion for undamped free vibrations of a uniform Euler–Bernoulli beam is obtained as [24]

$$EJ\frac{\partial^4\eta}{\partial\xi^4}+m\frac{\partial^4\eta}{\partial\xi^2}=0 \tag{4}$$

where $\eta(\xi,t)$ is the transverse displacement of the beam (at point ξ and time t) due to bending, EJ is the bending stiffness (it is the product of the young's modulus E and the second moment of the area J of the beam), and m is the mass per unit length of the beam (Fig. 5).

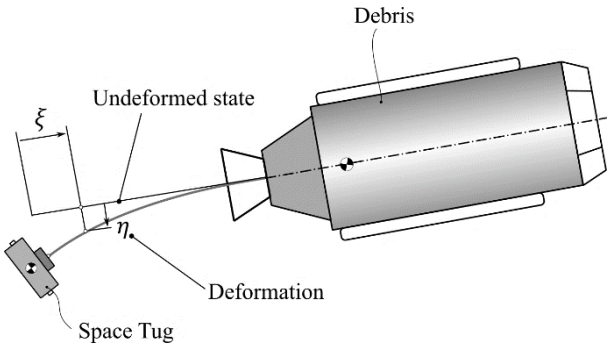

Fig. 5. Probe deformation

Boundary conditions for $\eta=0$ and $\eta=l$ are [25]:
for $\eta=0$ (attached mass and inertia)

$$\left(\frac{\partial^2\eta}{\partial\,\xi^2}=-\beta_{11}\,\frac{\partial^3\eta}{\partial\xi\,\partial t^2}\right)_{\xi=0}$$
$$\left(\frac{\partial^3\eta}{\partial\,\xi^3}=\beta_{12}\,\frac{\partial^2\eta}{\partial t^2}\right)_{\xi=0} \tag{5}$$

for $\eta=l$ (attached mass and inertia)

$$\left(\frac{\partial^2\eta}{\partial\,\xi^2}=-\beta_{21}\,\frac{\partial^3\eta}{\partial\xi\,\partial t^2}\right)_{\xi=l}$$
$$\left(\frac{\partial^3\eta}{\partial\,\xi^3}=\beta_{22}\,\frac{\partial^2\eta}{\partial t^2}\right)_{\xi=l} \tag{6}$$

where

$$\beta_{11}=\frac{J_1}{EJ},\qquad \beta_{12}=\frac{m_1}{EJ} \tag{7}$$

and

$$\beta_{21}=\frac{J_2}{EJ},\qquad \beta_{22}=\frac{m_2}{EJ} \tag{8}$$

m_1, m_2 are masses of the space tug and debris respectively, J_1, J_2 are moments of inertia of the space tug and debris.

The deflection of the probe is represented as [24]

$$\eta=\Phi(\xi)q(t) \tag{9}$$

where $\Phi(\xi)$ is the shape function

$$\Phi(\xi)=C_1\cos\frac{\lambda}{L}\xi+C_2\cosh\frac{\lambda}{L}\xi+C_3\sin\frac{\lambda}{L}\xi+C_4\sinh\frac{\lambda}{L}\xi \tag{10}$$

and

$$q(t)=a\cos\omega t+b\cos\omega t \tag{11}$$

where

$$\lambda^4=\omega^2\frac{ml^4}{EJ} \tag{12}$$

ω is the beam oscillation frequency. From the first two boundary conditions (5) we can express the unknown constants C_1, C_2

$$C_1=\frac{(C_3-C_4)l\,m}{2\,\lambda\,m_1}-\frac{(C_3+C_4)\,J_1\lambda^3}{2EJ\,l^3m} \tag{13}$$

$$C_2=\frac{(C_3-C_4)l\,m}{2\,\lambda\,m_1}+\frac{(C_3+C_4)\,J_1\lambda^3}{2EJ\,l^3m} \tag{14}$$

After substituting (13) into (6) we get the system of linear equation for C_3 and C_4

$$\begin{pmatrix}a_{11} & a_{12}\\ a_{21} & a_{22}\end{pmatrix}\begin{pmatrix}C_3\\ C_4\end{pmatrix}=\begin{pmatrix}0\\0\end{pmatrix} \tag{15}$$

where

$$\begin{aligned}a_{11}=\frac{1}{2\,EJ\,l^3mm_1}\big(&EJ\,l^7m^3(-\cos\lambda+\cosh\lambda)\\&+l^3m\lambda(-2\mathrm{EJ}l^3m\sin\lambda\\&+\lambda^3(\cos\lambda+\cosh\lambda)J_1)m_1\\&+\lambda^3J_2(EJ\,l^4m^2(\sin\lambda-\sinh\lambda)\\&-\lambda(2EJ\,l^3m\cos\lambda+\lambda^3(\sin\lambda+\sinh\lambda)J_1)m_1)\big)\end{aligned} \tag{16}$$

$$a_{12} = \frac{1}{2\,EJ\,l^3 m m_1}(EJ\,l^7 m^3(\cos\lambda - \cosh\lambda) + l^3 m\lambda(2EJ\,l^3 m\sinh\lambda + \lambda^3(\cos\lambda + \cosh\lambda)J_1)m_1 + \lambda^3 J_2(EJ\,l^4 m^2(-\sinh\lambda + \sinh\lambda) - \lambda(2EJ\,l^3 m\cosh\lambda + \lambda^3(\sin\lambda + \sinh\lambda)J_1)m_1)) \quad (17)$$

$$a_{21} = \frac{1}{2EJ\,l^3 m m_1}\Big(EJl^4 m^2(lm(\sin\lambda + \sinh\lambda) + \lambda(\cos\lambda + \cosh\lambda)m_2) + \lambda m_1\big(\lambda^3 J_1(lm(-\sin\lambda + \sinh\lambda) + \lambda(-\cos\lambda + \cosh\lambda)m_2) + 2\,EJ\,l^3 m(-lm\cos\lambda + \lambda\sin\lambda\, m_2)\big)\Big) \quad (18)$$

$$a_{22} = \frac{1}{2\,EJ\,l^3 m m_1}(-EJl^4 m^2(lm(\sin\lambda + \sinh\lambda) + \lambda(\cos\lambda + \cosh\lambda)m_2) + \lambda m_1(\lambda^3 J_1(lm(-\sin\lambda + \sinh\lambda) + \lambda(-\cos\lambda + \cosh\lambda)m_2) + 2\,EJ\,l^3 m(lm\cosh\lambda + \lambda\sinh\lambda\, m_2))) \quad (19)$$

To obtain non-trivial solution for C_3 and C_4 the determinant of the coefficient matrix should be equal to zero

$$\begin{vmatrix} a_{11} & a_{12} \\ a_{21} & a_{22} \end{vmatrix} = 0 \quad (20)$$

For given system parameters m, l, m_1, m_2, EJ, J_1 and J_2, one can solve for the roots of Eq. (20) and get the eigenvalues of the system

$$\lambda_1, \lambda_2, \lambda_3, \ldots \lambda_N \quad (21)$$

For each eigenvalue λ_i the undamped frequency of free oscillations can be obtained using (12)

$$\omega_i = \frac{EJ}{m\,l^4}\lambda_i^2 \quad (22)$$

Shape function is obtained for each eigenvalueλ_i within constant factor C_{3i}

$$\Phi(\xi,\lambda_i) = C_{1i}\cos\frac{\lambda_i}{L}\xi + C_{2i}\cosh\frac{\lambda_i}{L}\xi + C_{3i}\sin\frac{\lambda_i}{L}\xi - C_{3i}\frac{a_{11}}{a_{12}}\sinh\frac{\lambda_i}{L}\xi \quad (23)$$

where the constants C_{1i}, C_{2i} are obtained from (13) and (14) as functions of λ_i and C_{3i}, taking into account that

$$C_{4i} = -C_{3i}\frac{a_{11}}{a_{12}} \quad (24)$$

Deformation of the probe is expressed as a linear combination of the contributions from all vibration modes:

$$\eta(\xi,t) = \sum_{i=1}^{\infty}\Phi(\xi,\lambda_i)(a_i\cos\omega_i t + b_i\sin\omega_i t) \quad (25)$$

The unknown constants a_i and b_i can be solved for using the initial conditions

$$\eta(\xi,0) = \sum_{i=1}^{\infty}\Phi(\xi,\lambda_i)\,a_i \quad (26)$$

and

$$\left(\frac{d\,\eta(\xi,t)}{dt}\right)_{t=0} = \sum_{i=1}^{\infty}\Phi(\xi,\lambda_i)\,\omega_i\,b_i \quad (27)$$

4. Simulation result

4.1 Parameters of the system and initial conditions

Here we consider docking process with two probe length:

1) Short and stiff probe
   $l = 5$ m, $EJ = 30680$ Nm^2
2) Long and flexible probe
   $l = 10$ m, $EJ = 1900$ Nm^2

Parameters of the space debris and space tug are presented in Table 1.

Table 1. Parameters of the system

Parameter	Value
m_1, kg	150
m_2, kg	1500
J_1, kgm^2	100
J_2, kgm^2	3000
Initial length of the probe, l_0, m	10 m
Initial angular velocity of the debris, ω_0, deg/s	10
EJ, Nm^2	1900
c_N, N/m	10^8

4.2 Docking stage

The integration process starts when the tip of the probe crosses the section of the nozzle of the debris. The axis of the tug is parallel to the axis of the space debris and the distance between the axes of the debris and space tug is $y_0 = 1$ m. Initial velocity V_0 of the space tug relative to the debris is 2 m/s. The angular velocity of the debris relative to the transverse axis is ω_0 =10 deg/s (Fig. 6).

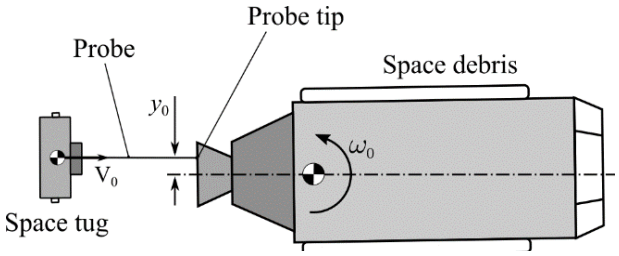

Fig. 6. Initial condition of the system

Fig. 7 shows the time history of the angular acceleration of the space tug during the first contact of the probe tip with the nozzle of the space debris. The angular acceleration of the space tug with the short and stiff probe is much higher than the angular acceleration of the space tug with long flexible probe (dashed lune). Angular acceleration of the tug with 10 m probe is less than 50 deg/s^2. Angular acceleration of the space tug with 5 m probe is 520 deg/s^2.

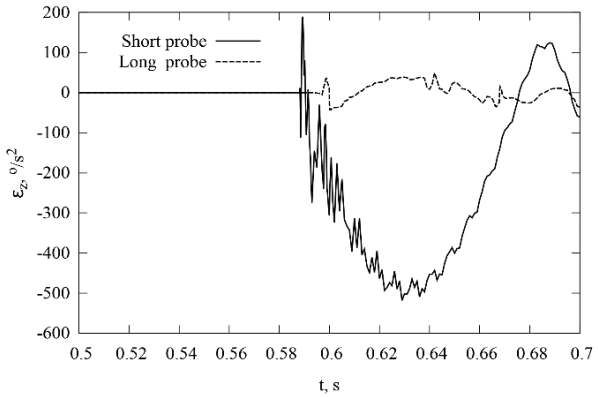

Fig. 7. Angular acceleration of the space tug during docking process for case 1 and 2

The obtained results confirm the assumption of less load on the tug construction when docked using a long probe for docking.

4.3 Probe retraction stage

At the third stage, the space *tug* retracts the flexible probe to dock with the debris. First four frequencies obtained from (20) are presented in Table 2. Note the obvious increasing of the frequencies with shortening the probe length.

Table 2. Natural frequencies of the probe

i	*l=5* м	*l=6* м	*l=7* м	*l=8* м	*l=9* м	*l=10* м
1	0.321	0.395	0.412	0.411	0.403	0.392
2	27.15	18.80	13.79	10.55	8.34	6.75
3	89.21	61.45	44.95	34.33	27.08	21.92

Fig. 8 and Fig. 9 show the first three shape functions of the probe when its length is equal to 10 m and 5 m. Note that the shape functions for $l = 5$ m and for $l = 10$ m differ slightly from each other.

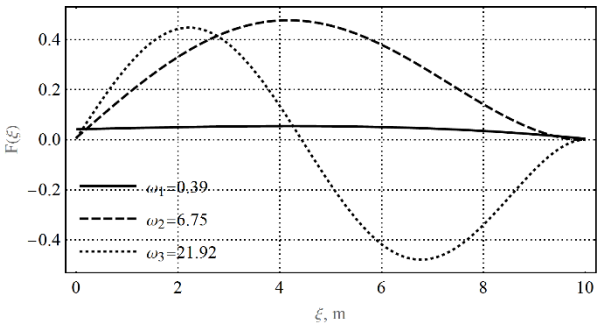

Fig. 8. First three shape functions of the flexible probe for length $l = 10$ m

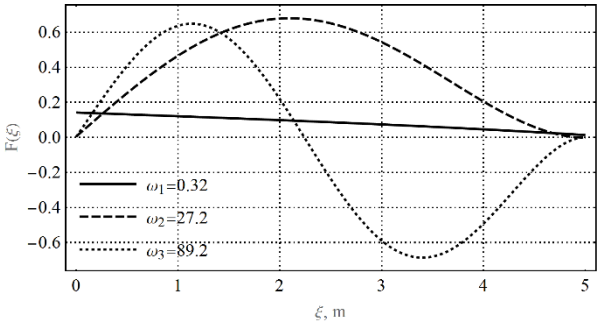

Fig. 9. First four shapes of the flexible beam for length $l = 5$ m

Fig. 10 shows deformation in the middle of the probe when its length is equal to 10 m.

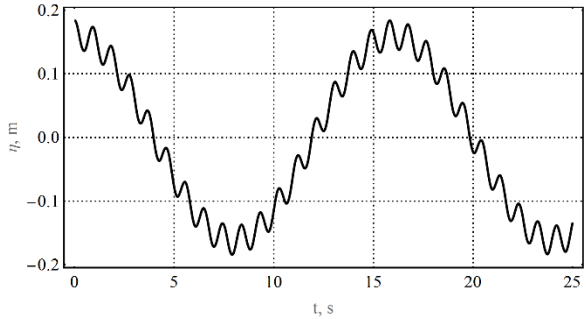

Fig. 10. – Deformation of the middle of the probe ($l = 10$ m)

Fig. 11 shows deformation of the probe in the middle of the probe when the length of the flexible probe is equal to 5 m.

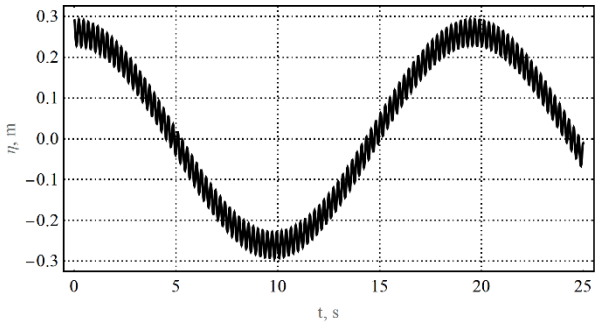

Fig. 11. – Deformation of the middle of the probe ($l = 5$ m)

Acceleration of the probe points results in dynamic inertia loads. It is quite expected that the frequency of the probe oscillations is increased with the decreasing of the probe length. Fig. 12 demonstrates how the acceleration of the middle of the probe depends on the probe length.

Increasing the acceleration of the probe during the retraction phase can led to the destruction of the probe so the oscillations of the probe should be damped.

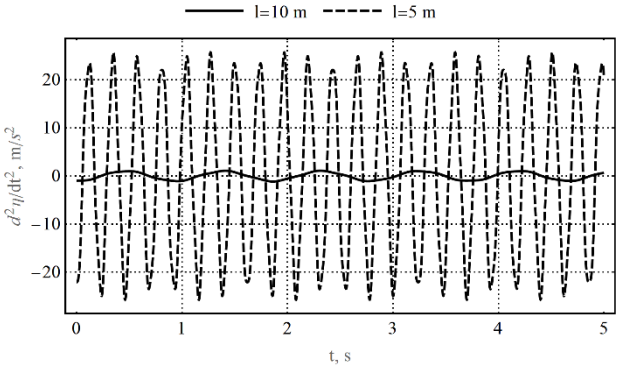

Fig. 12. – Acceleration of the middle of the probe for $l = 5$ m and $l = 10$ m

5. Conclusions

It is shown that using long flexible probe to dock with the tumbling debris object can decrease the contact impact force on the space tug. Here we pointed out the problems of using long flexible probe to dock with an uncooperative orbital stage type space debris object. Future investigations will continue to improve the mathematical model of the docking process and the beam retracting process. It is planned to develop a universal mathematical model based on FEM method suitable for the describing the docking process and the stage of retraction of the elastic probe of varying cross section area and for solving the problem of stabilizing the relative transverse and torsional vibrations of the tug and debris with decreasing the length of the probe.

Acknowledgements

This study was supported by the Russian Science Foundation (Project No. 16-19-10158)

References

[1] C. Bonnal, J.-M. Ruault, M.-C. Desjean, Active debris removal: Recent progress and current trends, Acta Astronaut. 85 (2013) 51–60. doi:10.1016/j.actaastro.2012.11.009.

[2] V.S. Aslanov, V. V. Yudintsev, Dynamics of large space debris removal using tethered space tug, Acta Astronaut. 91 (2013) 149–156. doi:10.1016/j.actaastro.2013.05.020.

[3] V.S. Aslanov, V. V. Yudintsev, Behaviour of tethered debris with flexible appendages, Acta Astronaut. 104 (2014) 91–98. doi:10.1016/j.actaastro.2014.07.028.

[4] R. Benvenuto, M. Lavagna, Flexible Capture Devices for Medium To Large Debris Active Removal: Simulations Results To Drive Experiments, Robotics.Estec.Esa.Int. (2013).

[5] E.M. Botta, I. Sharf, A.K. Misra, M. Teichmann, On the simulation of tether-nets for space debris capture with Vortex Dynamics, Acta Astronaut. 123 (2016) 91–102. doi:10.1016/j.actaastro.2016.02.012.

[6] E.M. Botta, I. Sharf, A.K. Misra, Contact Dynamics Modeling and Simulation of Tether Nets for Space-Debris Capture, J. Guid. Control. Dyn. 40 (2016) 1–14. doi:10.2514/1.G000677.

[7] V.S. Aslanov, V. V. Yudintsev, Dynamics, analytical solutions and choice of parameters for towed space debris with flexible appendages, Adv. Sp. Res. 55 (2015) 660–667. doi:10.1016/j.asr.2014.10.034.

[8] V.S. Aslanov, V. V. Yudintsev, The motion of tethered tug-debris system with fuel residuals, Adv. Sp. Res. 56 (2015) 1493–1501. doi:10.1016/j.asr.2015.06.032.

[9] F. Aghili, Active Orbital Debris Removal Using Space Robotics, Robotics.Estec.Esa.Int. (2012). http://robotics.estec.esa.int/i-SAIRAS/isairas2012/Papers/Session 8B/08B_01_aghili.pdf (accessed April 20, 2014).

[10] L. Felicetti, P. Gasbarri, A. Pisculli, M. Sabatini, G.B. Palmerini, Design of robotic manipulators for orbit removal of spent launchers' stages, Acta Astronaut. 119 (2016) 118–130. doi:10.1016/j.actaastro.2015.11.012.

[11] H. Takehiro, N. Wataru, F. Ohmi, G. Kenta, U. Seiya, MOTION AND CONTROL OF DEBRIS CAPTURE WITH SUPER MULTI-LINK SPACE MANIPULATOR, in: Proc. 65th Int. Astronaut. Congr., 2014: pp. 1–7.

[12] R. Benvenuto, S. Salvi, M. Lavagna, Dynamics analysis and GNC design of flexible systems for space debris active removal, Acta Astronaut. 110 (2015) 247–265. doi:10.1016/j.actaastro.2015.01.014.

[13] G. Zhai, Y. Qiu, B. Liang, C. Li, On-orbit capture

with flexible tether–net system, Acta Astronaut. 65 (2009) 613–623. doi:10.1016/j.actaastro.2009.03.011.
[14] M.R. Lavagna, R. Armellin, A. Bombelli, R. Benvenuto, R. Carta, Debris Removal Mechanism Based on Tethered Nets, in: iSAIRAS Int. Symp. Artif. Intell. Robot. Autom. Sp., 2012.
[15] V.S. Syromyatnikov, Docking devices of space vehicles, Mashinostroenie, Moscow, 1984.
[16] W. Fehse, Automated Rendezvous and Docking of Spacecraft, System. (2003). doi:10.1017/CBO9780511543388.
[17] V.I. Trushlyakov, Y.T. Shatrov, I.I. Oleynikov, Y.N. Makarov, E.A. Yutkin, The method of docking spacecraft, RU 2521082, 2010. http://www.findpatent.ru/patent/252/2521082.html.
[18] W.P. Alfred, L.R. William, Method and Apparatus for Securing To a Spacecraft, 3508723, 1970.
[19] C.K. Moody, A.B. Probe, A. Masher, T. Woodbury, M. Saman, J. Davis, J.E. Hurtado, Laboratory Experiments for Orbital Debris Removal, in: AAS Guid. Navig. Control Conf., Breckenridge, CO, 2016: pp. 1–12.
[20] X. Zhang, Y. Huang, X. Chen, Contact analysis of flexible beam during space docking process, Adv. Eng. Softw. 64 (2013) 38–46. doi:10.1016/j.advengsoft.2013.05.010.
[21] Z. Xiang, H. Yiyong, C. Xiaoqian, H. Wei, Modeling of a space flexible probe – cone docking system based on the Kane method, Chinese J. Aeronaut. 27 (2014) 248–258. doi:10.1016/j.cja.2014.02.020.
[22] W. Han, Y.Y. Huang, X. Zhang, X.Q. Chen, Collision Simulation Analysis for Space Flexible Probe-Cone Docking Mechanism, Appl. Mech. Mater. 138–139 (2011) 111–116. doi:10.4028/www.scientific.net/AMM.138-139.111.
[23] P. David S. F., Mir Hardware Heritage/Part 1 - Soyuz, 15 April 2014. (2014). https://en.wikisource.org/wiki/Mir_Hardware_Heritage/Part_1_-_Soyuz#cite_note-21.
[24] G. Kelly, Fundamentals of mechanical vibrations, McGraw-Hill, 2000. http://books.google.ru/books?id=yVjvAAAAMAAJ (accessed April 20, 2014).
[25] A. Erturk, D.J. Inman, Piezoelectric Energy Harvesting, 2011. doi:10.1002/9781119991151.